Design and Characterization of an External Cavity Diode Laser for NV^- Center Photoluminescence Excitation

John Raihala[1,2]

[1] *Institute of Nuclear Theory REU, University of Washington, Seattle, WA 98195*
[2] *Department of Physics, University of Chicago, Chicago, IL 60637*

The nitrogen vacancy (NV) center is a point defect in diamond which shows potential to be used as an electron spin qubit for quantum information processing systems. NV center photoluminescence plays an important role in manipulation and readout of spin states, as well as in the entanglement of NV center qubits. In this paper I describe the design and characterization of a tunable external cavity diode laser (ECDL) for future work characterizing the emission spectrum of NV center samples using photoluminescence excitation.

I. INTRODUCTION

At a high level, this project is motivated by the desire to develop a functional and efficient system for quantum computing. In classical computing, computations are performed using units of information called bits, which exist in one of two states at any given time. Quantum computing allows for the use of quantum bits, or qubits, which can exist in any superposition of two basis states. Also, unlike classical bits, qubits can be entangled. Theoretically, these features provide several advantages over classical computation. Quantum computing algorithms have been developed which improve on the asymptotic runtime of the fastest known classical algorithms for certain important problems–most notably, Shor's algorithm for the factorization of large integers. Quantum computing would also provide for secure communication with methods such as quantum key distribution, and would be useful for the efficient simulation of large quantum systems.

In theory, any two-level quantum system can be used as a qubit, and researchers in the field of quantum computing are exploring a variety of physical implementations for qubits: superconducting Josephson junction circuits, trapped ions, and solid state systems such as the NV center are several popular approaches.

II. NV CENTER QUBITS

The NV center is a point defect in diamond in which one carbon atom is replaced with a nitrogen atom and an adjacent carbon atom is replaced with a vacancy. The NV center has several charge states; the NV^- charge state, with two unpaired electrons forming a spin S=1 system, is especially promising for its use as a qubit. The electron spin states can be manipulated by a number of means, including optical excitation in the visible range. The NV center ground states and excited states are split by 1.945 eV, corresponding to 637 nm light, and at sufficiently low temperatures the NV center has a sharp peak in its absorption and emission spectra (the zero phonon line, or ZPL) corresponding to this transition. If the qubit states $|0\rangle$ and $|1\rangle$ are encoded in the $m_s = 0$ and one of the $m_s = \pm 1$ ground states, optical excitation of the NV center with laser light on resonance with the ZPL can be performed for a number of purposes: preparation of the qubit state, readout of the qubit state using off-resonant photon emission, or entanglement of multiple NV center qubits using resonant emission. Entanglement of two distant NV^- center qubits using these methods has been demonstrated by a research group at Delft University of Technology in the Netherlands [1].

The ZPL photoluminescence is overall of great importance for the use of NV centers as qubits. However, the frequency of the ZPL varies somewhat from NV center to NV center. In our lab, a graduate student working with NV centers observed one sample with resonance at 637.3 nm, and another sample at 637.7 nm. Furthermore, the frequency of ZPL photons emitted by a given NV center will wander over time as a result of spectral diffusion, caused by extreme sensitivity to variations in local electric field, and ZPL broadening due to thermal effects.

In order to characterize the ZPL emission of an NV center, it is useful to have a tunable source of laser light for performing photoluminescence excitation. Repeatedly tuning the laser through the expected frequency range of the ZPL and detecting fluorescence from the NV center will yield a plot of resonant frequency over time. Such a plot is shown in Figure 1.

III. EXTERNAL CAVITY DIODE LASER

My work this summer, in collaboration with another student in Kai-Mei Fu's lab, focused on the construction and characterization of an external cavity diode laser (ECDL) for future work on NV center photoluminescence as described in Section II. We based the design of our laser on plans outlined by R. Scholten at the University of Melbourne. For detailed information regarding the laser design see [2].

The laser uses a broadband, antireflection coated laser diode (Sacher Lasertechnik SAL-0640-030) mounted in a collimating tube (Thorlabs LT110P-B) with an aspheric collimating lens (focal length f=6.24mm, AR coated for 650-1050nm). The beam is incident on a holographic

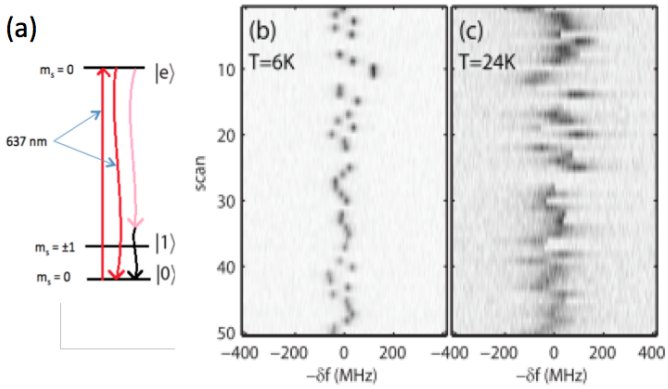

FIG. 1. a) An energy level diagram of the NV center qubit. The qubit states $|0\rangle$ and $|1\rangle$ are encoded in the ground states, and the $|0\rangle$ state is optically coupled to an excited state $|e\rangle$. b) and c) Plots showing the spectral diffusion and phonon broadening of resonant NV center emission, made by optically exciting the NV center on resonance with the $|0\rangle \rightarrow |e\rangle$ transition and observing the resulting photon emission [3].

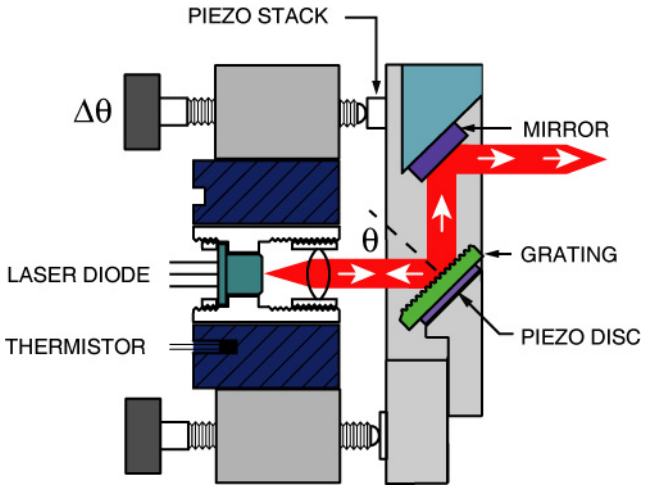

FIG. 2. ECDL diagram [2]. In our design we opted not to include the piezo disc mounted under the grating, which could be included to provide fine tuning of cavity length.

diffraction grating (Thorlabs GH13-18V, 1800 lines/mm) aligned such that the first order diffraction is coupled back to the laser diode, and the direct reflection off the grating is coupled out as the laser beam. This is called the Littrow configuration. The collimation tube is inserted into a modified Newport UPA-PA1 mirror mount adaptor, which is mounted on the back plate of a Newport U100-P2H mirror mount. The diffraction grating and a visual mirror are fixed to the modified front mirror plate. Figure 2 shows a diagram of this setup.

For low drive currents, the laser diode will exhibit broadband fluorescence. Figure 3 shows the diode's broadband spectrum at a low current. Note that it is centered at 640 nm with a FWHM of about 10 nm, or about 7 THz. Above a certain current–the lasing threshold–the

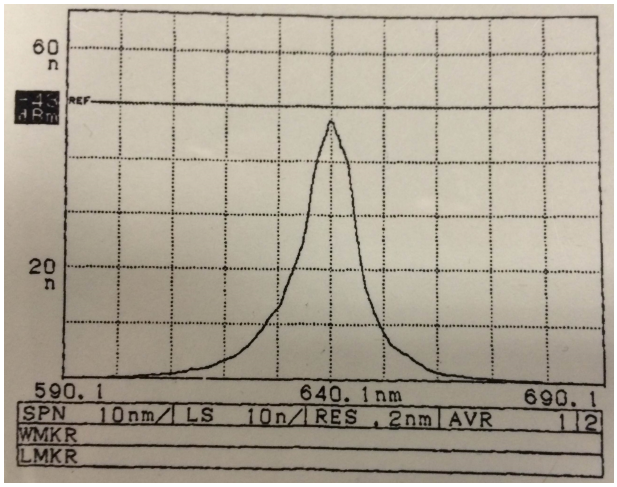

FIG. 3. Sacher laser diode spectrum without optical feedback. Central frequency is 640nm, FWHM is roughly 10nm. A lasing wavelength of 637nm is easier to achieve at lower currents, since at high currents the intensity peak at 640nm will compete with the 637nm cavity. The diode's antireflection coating mitigates this problem to a large extent.

diode will lase. However, when the laser diode is driven at a current just below the lasing threshold, it is very sensitive to optical feedback. In our setup, by adjusting the angle between the diode and the grating, it is possible to select the frequency of the first order diffraction that is fed back to the diode. If the optics are aligned properly, an optical cavity is formed between the diode and the grating, causing the diode to lase with a narrow linewidth spectrum centered at the frequency selected by the grating angle. The University of Melbourne group, using the same ECDL design, achieved a stable linewidth of less than 1 MHz [2].

In the Littrow configuration, where the angle of light incident on the diffraction grating is the same as the angle of the first order diffraction, the wavelength λ of light and the angle of incidence θ are related by the grating equation

$$\theta = arcsin(\frac{\lambda}{2d})$$

where d is the line spacing of the grating. For our grating with 1800 lines/mm, this gives an angle of about 35 degrees for 637 nm light. The aluminum grating mount is machined to 35 degrees in accordance with this calculation. Frequency tuning of the laser is achieved by slightly adjusting the grating angle, thus changing the portion of the diode's frequency spectrum which is diffracted back to the diode.

The θx adjustment screw provided with the mirror mount can be turned by hand for coarse tuning of the grating angle. Fine tuning of frequency is achieved by applying a voltage across a piezostack (Thorlabs AE0203D04F) mounted between the screw and its contact point on the mirror mount (see Figure 2). The length

of the piezostack changes in response to an applied voltage, allowing for high precision electronic adjustment of the grating angle.

The recommended drive voltage for the AE0203D04F piezo is 100 V, and the maximum drive voltage is 150 V. The displacement of the piezo should be approximately proportional to drive voltage, although some degree of hysteresis is expected. Thorlabs does not provide a plot of length change as a function of applied voltage, but reports that at 100 V the nominal displacement is $3.0 \pm 1.5\mu m$, and at 150 V it is $4.6 \pm 1.5\mu m$.

Assuming that the mirror plates are roughly parallel, and using the fact that the piezo actuator is located 37.5 mm from the mirror mount pivot point, simple trigonometry shows that a 3.0 μm displacement of the piezo will lead to a 0.0046°change in the grating angle. Using the grating equation above, we can write

$$\Delta\lambda = 2 \cdot d \cdot sin(\theta + \Delta\theta) - \lambda$$

which, for $\lambda = 637nm$ and $\Delta\theta = 0.0046°$, leads to a change in wavelength of $\Delta\lambda = 0.07nm$ or $\Delta\nu = 50GHz$.

Another limiting factor for the laser's tunability is the free spectral range (FSR) of the optical cavity–that is, the frequency spacing between longitudinal modes that are resonant with the cavity length. For our cavity length of roughly 15 mm, we expect the FSR to be about 10 GHz. Therefore the cavity FSR, rather than the piezo scan range, should be the limiting factor for the laser's tunability. Still, 10 GHz is sufficient for scanning across the expected worst-case single NV center emission line.

IV. LASER PERFORMANCE

For the laser to be useful for the characterization of NV center photoluminescence, it must maintain a high degree of frequency stability. Our goal was to achieve a linewidth on the order of 1MHz in order to resolve even the narrowest NV center emission lines (10 MHz). Along with proper adjustment of the collimating lens and grating angle, systems in place for temperature control and diode current control must be tuned in tandem to optimize frequency stability of the laser.

a. Temperature Stability Temperature control of the laser is very important for frequency stability. When the laser is not cooled, the temperature will rise dramatically as the laser generates heat, especially for high diode currents. In our setup, a Thorlabs TH10K thermistor is mounted near the diode and is used for monitoring the temperature of the laser. The temperature of the laser is stabilized using a thermoelectric cooler (Thorlabs TEC3-2.5) mounted between the top baseplate and the bottom baseplate of the laser. A layer of thermal grease applied at the interfaces between components ensures good thermal conductivity throughout the system. The TEC and thermistor in the laser can be connected to any temperature control unit intended to drive a TEC; we have used both a Thorlabs TED200C and a Thorlabs TCM1000T.

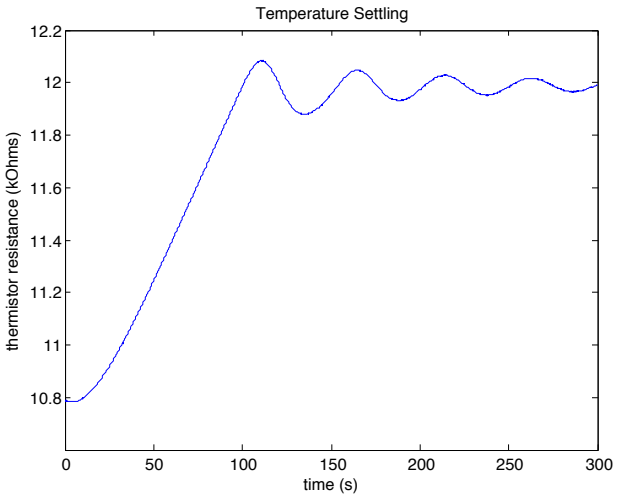

FIG. 4. Laser temperature settling to its setpoint. The amount of ringing can be reduced by adjusting the PID controls of the temperature control unit. If the PID controls are not properly adjusted, the temperature will oscillate indefinitely.

The Thorlabs TED200C provides long term temperature stability to within $\pm 1\Omega$, corresponding to $\pm 0.002°$ C. Figure 4 shows a five minute scan of the temperature while it was settling; after ten to fifteen minutes of settling, the temperature reached the expected accuracy of $\pm 0.002°$ C. Figure 5 shows a plot of laser frequency as a function of thermistor resistance as the laser approaches its set temperature–from this we calculated a frequency dependence on temperature of about 30 GHz/°C. This plot also shows a general trend we observed of poor frequency stability and frequent mode hops when the temperature is not held constant.

Since laser frequency is highly dependent on temperature, we predicted the existence of an optimal temperature or temperatures that would minimize frequency noise and mode hopping. The viable temperature range is determined on the low end by the dew point of the room (in our case 16°C), below which point condensation could cause damage to the laser, and on the high end by the requirement that the laser be at or below room temperature since the TEC is mounted with the cold side adjoining the laser. We monitored laser frequency stability at a range of temperatures between 18 and 22 °C, but were unable to determine whether there is an optimal temperature setpoint for laser performance. It is probably the case that the optimal temperature depends on other factors of laser alignment, including diode current and grating angle, and that the most important factor is whether the laser frequency is tuned to the middle of a free spectral range so as to minimize mode hopping.

b. Frequency Stability With the laser held at a constant temperature, the diode current can be adjusted to

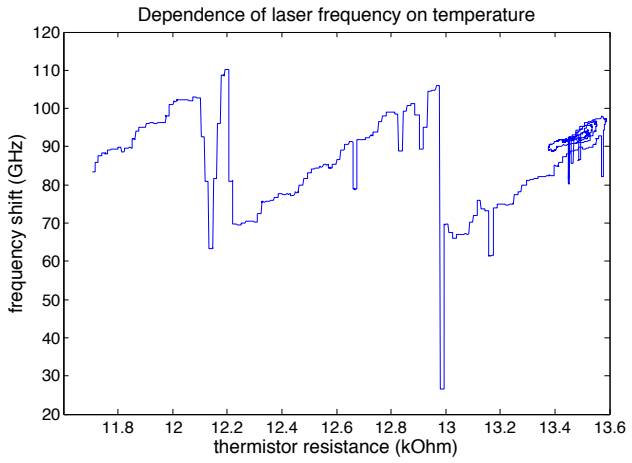

FIG. 5. Laser frequency vs temperature as the thermistor approaches its setpoint of 13.5 kΩ. Two persistent mode hops and a number of transient mode hops occur–why these mode hops are around 40 GHz instead of the 8-12 GHz observed elsewhere remains unclear. From this plot we determined a frequency dependence on temperature of 30 GHz/°C.

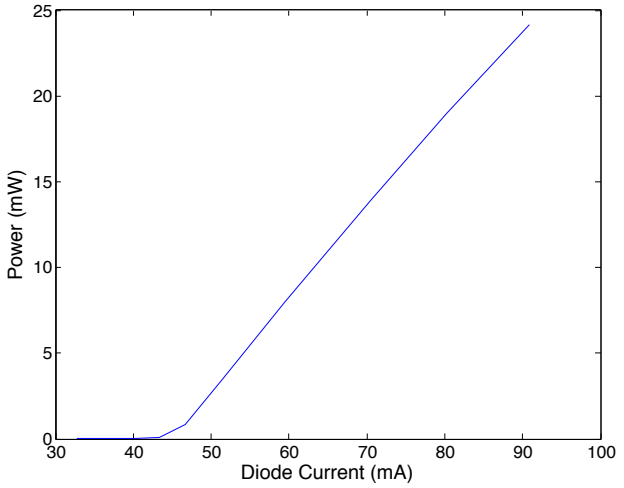

FIG. 6. Laser power as a function of diode current. Measurements were made using a Newport 2832-C power meter.

further optimize power output and frequency stability. Figure 6 shows a plot of measured power as a function of diode current. The power output of the laser will be very low (1-100 μW) when the diode is fluorescing at a current below the lasing threshold (the lasing threshold is nominally 33mA with feedback or 46mA without feedback; we have observed a threshold around 46mA with feedback, and have not done sufficient testing without feedback to report a lasing threshold). Above this threshold, power will increase linearly with current, up to the 25-35mW range for an input current around 90mA.

The amount of frequency noise and the rate at which

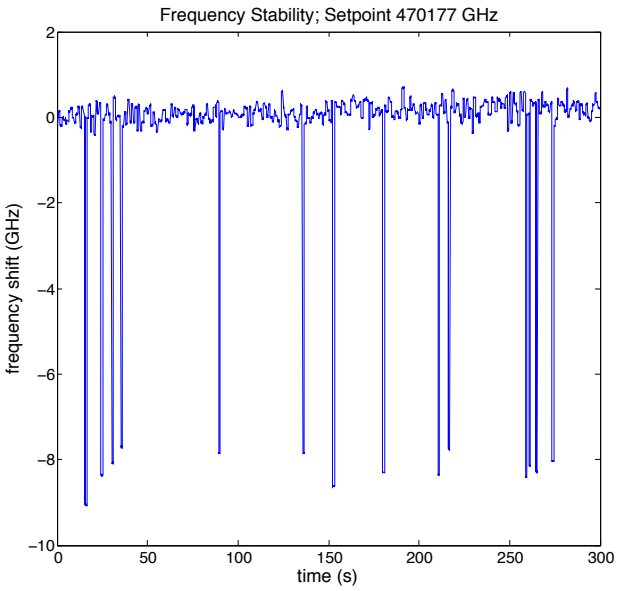

FIG. 7. Laser frequency stability over a period of five minutes at a diode current of 65mA, showing mode hops of around 8 GHz and frequency noise on the order of 500 MHz.

mode hops occur both depend to a large degree on diode current. The laser is most sensitive to optical feedback just below the lasing threshold without feedback, and can be made to demonstrate good frequency stability at the desired wavelength of 637 nm for diode currents in the 40-50 mA range. As current is increased past a certain point, we have observed mode hops become more frequent until the laser makes a persistent hop to a wavelength of 639-640 nm, the intensity maximum of the laser diode without optical feedback. Beyond this point frequency stability is good, but the laser is no longer at the desired wavelength.

Figure 7 shows a plot of laser frequency over time with the diode current set to 65 mA. The frequency of 470177 GHz corresponds to 637.6 nm. Mode hops of around 8 GHz occur fairly regularly, although the frequency quickly returns to its setpoint. In other trials we consistently observed mode hops in the 8-12 GHz range, corresponding in size to the expected free spectral range of the laser cavity. Along with the mode hops, there appears to be several hundred MHz noise. Figure 8 shows a plot of laser frequency with the diode current set to 91 mA. In this case there are no mode hops and the apparent frequency noise is reduced to roughly 100 MHz, but the wavelength has jumped to 639.6 nm.

All of our measurements of laser frequency were performed using a Burleigh WA-1500 Wavemeter, which has a nominal frequency accuracy of 0.2 ppm, or about 100 MHz. As a result, our observation of 100 MHz frequency noise might be an artifact of the measurement apparatus, and more precise tests would need to be performed in order to completely characterize the performance of our

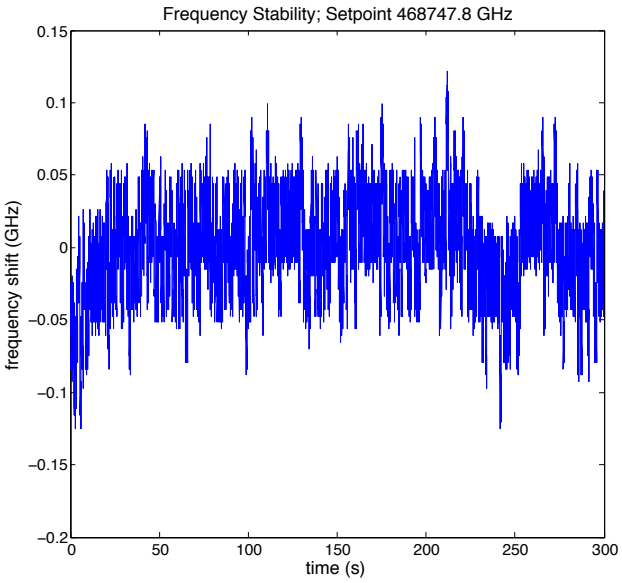

FIG. 8. Laser frequency stability over a period of five minutes at a diode current of 91mA, showing no mode hops and frequency noise on the order of 100 MHz.

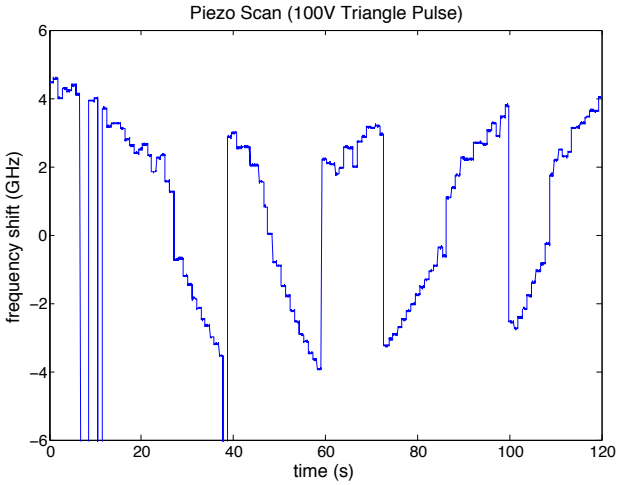

FIG. 9. Laser frequency change in response to 100V triangle pulse on piezostack. Persistent mode hops occur at 40, 60, 70, and 100 seconds; the largest mode hop free scan range is 7 GHz.

laser. We can however put an upper limit of 100 MHz on the laser's frequency noise when temperature, grating angle, and diode current are all properly tuned.

c. Piezo Performance In addition to characterizing our laser's frequency stability with no voltage applied to the piezostack, we performed measurements of frequency as a function of piezo voltage in order to determine the actual scanning range of our laser. As discussed in Section III, we expect a 100 V DC signal to correspond to a $3.0\mu m$ displacement of the piezo, which we expect to lead to a 50 GHz shift in laser frequency. Unfortunately, we have observed an inconsistent scan range when ramping the piezo through 100 V, with at best a 15 GHz range. Over this 15GHz range the laser mode hops several times. The biggest mode hop free scanning range we have observed during these tests is about 7 GHz. Figure 9 shows a plot of frequency over time as the piezo voltage was ramped at a constant rate from 0 to 100 V and back. The piezo voltage was driven using a voltage amplifier built by another student in the lab, which was in turn driven by the analog output of a National Instruments DAQ unit.

In addition to these 100 V piezo scans, we also performed 30 V scans using a commercial 40 V voltage source. For a 30 V signal, where we would expect a roughly 16 GHz scan range, we instead observed scanning ranges between 2 and 5 GHz. Fortunately, it is usually possible to make this 2-5 GHz scan range mode hop free. Figure 10 shows a plot of frequency over time as the piezo voltage was manually tuned from 0 V to 30 V.

We hypothesize that the discrepancies between expected scan range and observed scan range may be a result of a broken piezo, improper mounting of the piezo, or a noisy voltage source. Potential improvements could include epoxying the piezo in place for a more reliable mechanical connection, and incorporating feedback between the piezo voltage and diode current control for increased frequency stability.

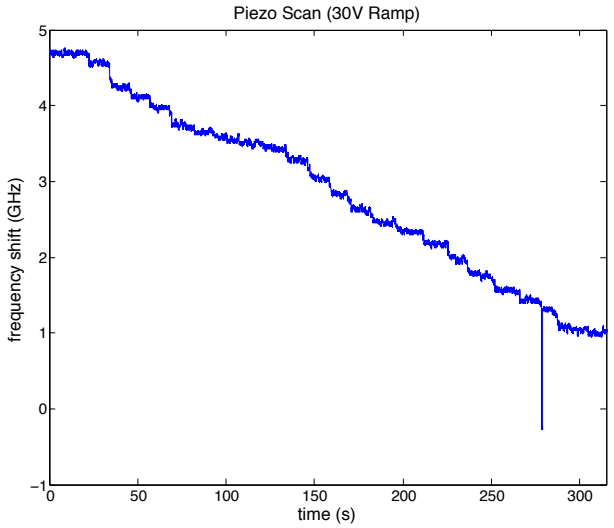

FIG. 10. Laser frequency change in response to 30V ramp on piezostack. No persistent mode hops occur, but the scan range is less than 4 GHz.

V. CONCLUSIONS

We have constructed a tunable external cavity diode laser for use in future experiments with NV^- centers, and have demonstrated that the laser has a linewidth of at most 100 MHz. The laser can currently be tuned by several GHz by applying a voltage to the piezostack used for fine adjustment of the diffraction grating angle. Further work should be done to make more precise measurements of the laser linewidth and to increase the frequency tuning range.

Future measurements of laser frequency noise should be performed using a Fabry-Perot etalon rather than the Wavemeter. We have an etalon in the lab with an inherent transmission peak linewidth of 27 MHz, so our upper bound of 100 MHz on laser linewidth could potentially be lowered to 27 MHz by simply coupling the laser into the etalon and monitoring the power transmitted. The exact frequency linewidth could be determined by making more sensitive measurements of fluctuations in power transmission with the laser tuned to the steepest slope of the etalon transmission curve, ideally yielding the desired result of less than 1 MHz noise.

If necessary, frequency stability could be improved by further isolating the laser from sources of vibration. Instead of being mounted directly to the optics table, the laser could instead be mounted to an optical breadboard isolated from the table by strips of a vibration-damping material such as Sorbothane. Laboratory equipment such as oscilloscopes and voltage supplies could be moved off of the optics table. More work could also be done to determine the optimal settings for laser temperature and diode current.

Tuning the laser electronically with the piezostack has not given us the desired frequency scanning range. One potential improvement would be to mount the piezostack in place with epoxy. If this does not improve the laser tuning range, either the voltage source or the piezo itself should be replaced.

ACKNOWLEDGMENTS

I would like to thank my mentor, Kai-Mei Fu, for providing guidance throughout the summer. I would also like to thank Kevin Jamison, another undergraduate with whom I worked closely on this project, and the rest of Fu lab for their assistance and support. Deep Gupta, Alejandro Garcia, Shih-Chieh Hsu, Gray Rybka, Linda Vilett, and Janine Nemerever all did an excellent job in organizing the INT REU program. Finally, I would like to thank the NSF for funding.

[1] H Bernien, B Hensen, W Pfaff, G Koolstra, M S Blok, L Robledo, T H Taminiau, M Markham, D J Twitchen, L Childress, and R Hanson. Heralded entanglement between solid-state qubits separated by 3 meters. *Nature*, 479:86–90, 2013.

[2] C J Hawthorn, K P Weber, and R E Scholten. Littrow configuration tunable external cavity diode laser with fixed direction output beam. *Review of Scientific Instruments*, 72(12):4477–4479, 2001.

[3] C Santori, P E Barclay, K-M C Fu, R G Beausoleil, S Spillane, and M Fisch. Nanophotonics for quantum optics using nitrogen-vacancy centers in diamond. *Nanotechnology*, 21, 2010.